PERGAMON

Pattern Recognition 32 (1999) 2029–2039

PATTERN RECOGNITION
THE JOURNAL OF THE PATTERN RECOGNITION SOCIETY

www.elsevier.com/locate/pattcog

A study on the dual vanishing point property☆

Jen-Bin Huang[a], Zen Chen[a,*], Jenn-Yih Lin[b]

[a]*Institute of Computer Science and Information Engineering, National Chiao Tung University, Hsinchu, Taiwan 30050, Republic of China*
[b]*Electrical Engineering Department, Ming-Hsin Institute of Technology, Hsinchu, Taiwan, Republic of China*

Received 17 February 1997; received in revised form 7 December 1998; accepted 7 December 1998

Abstract

Vanishing points and vanishing lines are useful information in computer vision. In this study, an interesting dual property of vanishing point is first introduced. Next, we point out that there also exists a dual property of vanishing line. With the dual vanishing point and vanishing line properties, some 3D intersection inference can be made based on their image lines. Two applications are given to illustrate the usage of the new results. The first one is to derive the 3D pose determination of a circle using two parallel image lines. The second one uses six specially designed 3D lines to adjust the cameras with respect to a fixture in a binocular vision system such that the resultant camera coordinate axes become parallel. © 1999 Pattern Recognition Society. Published by Elsevier Science Ltd. All rights reserved.

Keywords: Dual vanishing point; Dual vanishing line; 3D Coplanar lines; Parallel image lines; True or false intersection

1. Introduction

Line segments are reliable feature [1]. The reasons are that (1) lines are not easily affected by occlusion, (2) a line can achieve subpixel accuracy, and (3) the feature correspondence problem is easier and less ambiguous. Thus, lines are often used in computer vision, pattern recognition, scene matching, and image understanding, etc. In these fields, determining the relationship between the 2D image and the 3D object is a challenging task. One important property used frequently is the vanishing point. This property is about the perspective projection of parallel lines in the 3D space [2–5]. Many researchers used vanishing points in automatic manufacturing, vehicle navigation [6,7], object recognition [8], object reconstruction [9], and camera calibration [10,11], etc. According to the vanishing point property, perspective projections of several parallel 3D object lines meet at a vanishing point on the image plane [5] if the 3D lines are not parallel to the image plane. In this study, we infer the 3D information of parallel image lines. In this reverse manner, the dual property of the vanishing point, called the *dual vanishing point property*, is investigated and we obtain several properties in perspective geometry. This property shows that the corresponding 3D lines, which are assumed to belong to an object plane, of the parallel image lines generally intersect at a point. We refer to the intersection point as the 3D *inferred intersection point* (IIP). Moreover, the line defined by the 3D IIP and the center of projection (COP) is parallel to the parallel image lines.

Next, we examine the 3D IIPs on an object plane for inferring the 3D line information from multiple groups of parallel image lines. We point out that these IIPs will lie on a common line. Since this phenomenon is like the vanishing line property, we called it the *dual vanishing line property*. Several related properties are also given in this study.

☆This research was partially supported by the National Science Council of the Republic of China under Grant NSC84-2213-E009-047.

*Corresponding author. Tel.: 886-3-5731875; fax: 886-3-5723148.

E-mail address: zchen@csie.nctu.edu.tw (Z. Chen)

0031-3203/99/$20.00 © 1999 Pattern Recognition Society. Published by Elsevier Science Ltd. All rights reserved.
PII: S0031-3203(99)00002-3

With the dual vanishing point and vanishing line properties, some 3D line properties can be found from their corresponding image lines, namely, line parallelism or line intersection properties. Although the observed 2D image line properties are not adequate for the recovery of the corresponding 3D line equation, yet the dual vanishing point and line properties can be useful. We shall give two applications of these dual properties. One is to demonstrate the use of this new theory in the 3D pose determination of a circle using a set of two parallel image lines. In this application the pose parameters can be solved directly without transferring the circle image (an ellipse) into a circular shape as in the method by Kanatani and Liu [12]. Thus it simplifies the solving process. In the second application, a novel camera calibration method for a standard binocular vision system using six 3D lines in a specially designed configuration is given. The organization of the paper is as follows. Sections 2 and 3 present the dual properties. Section 4 addresses the various intersection configurations of 2D image lines corresponding to two or more coplanar or non-coplanar 3D lines. Sections 5 and 6 give two applications of the dual properties. Finally, Section 7 is the conclusion.

2. The dual vanishing point property

In the following, we first study the dual vanishing point property through geometric reasoning of parallel lines on the image plane. Assume the corresponding 3D lines of the parallel image lines belong to an object plane.

Theorem 1. *If two parallel lines l_1 and l_2 on the image plane are not parallel to a 3D object plane W and the COP (point G) is not on plane W, then*

(a) *lines l_1 and l_2 lead to a 3D IIP (H) on plane W, that is, their corresponding 3D lines L_1 and L_2 will intersect at a point (H), when extended.*
(b) *line $\overline{GH}$ is parallel to l_1 and l_2.*

Proof. As depicted in Fig. 1, line l_1 and point G define a plane P_1, and line l_2 and point G define a plane P_2. Since l_1 and l_2 are parallel image lines and G is on both planes P_1 and P_2, planes P_1 and P_2 intersect at a line, say L_G, that passes through point G.[1]

(a) To show lines L_1 and L_2 have an intersection point (i.e., 3D IIP): Lines L_1 and L_2 are the intersection lines of plane P_1 and plane W and of plane P_2 and plane W, respectively. Since planes P_1, P_2, and W are not parallel,

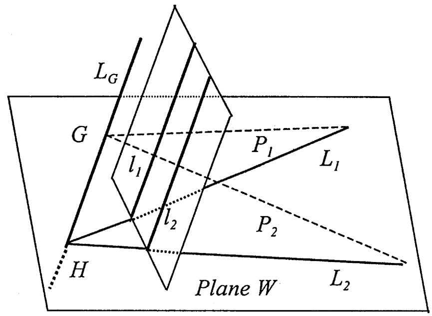

Fig. 1. The dual vanishing point property.

they intersect at a point (H). Point H must be the intersection point between line L_G and plane W. It is the intersection point between lines L_1 and L_2, i.e., the IIP.

(b) To show line $\overline{GH}$ is parallel to l_1 and l_2: We already know that $\overline{GH}$ and l_1 are on plane P_1 and that $\overline{GH}$ and l_2 are on plane P_2. Assume that $\overline{GH}$ is not parallel to lines l_1 and l_2, then $\overline{GH}$ intersects l_1 and l_2 at points E and F, respectively. Since line $\overline{GH}$ intersects two lines l_1 and l_2 on the image plane at two points, it must lie on the image plane. This is a contradiction to the fact that point G is not on the image plane. Thus, $\overline{GH}$ is parallel to lines l_1 and l_2. This also implies $\overline{GH}$ is parallel to the image plane. □

Let the X and Y axes of the camera (X–Y–Z) coordinate system be parallel to the x and y axes of the image (x–y) plane; the Z axis is the optical axis of the camera. Also let point G and the origin of the image plane be at (0, 0, 0) and $(0, 0, f)$, respectively. Given the equation of plane W, conventionally one may estimate the 3D IIP for image lines as follows. The backprojection planes defined by the parallel image lines and the COP are calculated. They intersect plane W at two object lines. The intersection point of the two object lines can then be computed. Here based on Theorem 1, Lemma 1 gives a simpler method.

Lemma 1. *Let the equations of parallel image lines l_1 and l_2 be $px + qy + r_i = 0, i = 1, 2, p^2 + q^2 \neq 0$, and the object plane equation of W be $AX + BY + CZ + D = 0$, then the 3D IIP, H, on the plane W is at $(-qD/(qA - pB), pD/(qA - pB), 0)$.*

Proof. According to Theorem 1, the 3D IIP of the parallel image lines is the intersection point of the plane W and the line $\overline{GH}$. Thus if both p and q are not equal to zero, the 3D IIP (X_0, Y_0, Z_0) satisfies both equations $AX + BY + D = 0$ and $X/q = Y/(-p)$ since $Z = 0$. As

[1] The authors would like to thank Dr. Jong-Quan (Karen) Lu, Schlumberger Austin Systems Center, Austin, Texas, for her contribution to the proof of Theorem 1.

a result, $X_0 = -qD/(qA - pB)$, $Y_0 = pD/(qA - pB)$, and $Z_0 = 0$. On the other hand, if p is zero (q will not be zero in such a case since $p^2 + q^2 \neq 0$), $\overline{GH}$ will be the X-axis, thus $X_0 = -D/A, Y_0 = 0$, and $Z_0 = 0$. Similarly, if q is zero, $\overline{GH}$ is the Y-axis, thus $X_0 = 0$, $Y_0 = -D/B$, and $Z_0 = 0$. If both A and B are equal to zero, plane $W(Z = -D/C)$ is parallel to the image plane, the 3D corresponding lines are parallel and the IIP is at infinity. In summary,

$$X_0 = \frac{-qD}{qA - pB}, \qquad Y_0 = \frac{pD}{qA - pB} \qquad \text{and} \qquad Z_0 = 0.$$

This lemma also makes it easier to estimate the equations of 3D object lines. According to the equation of parallel lines, the backprojection planes are $pX + qY + (r_i/f)Z = 0$, where f is the effective focal length of the camera. The direction cosines (N_{Xi}, N_{Yi}, N_{Zi}) of the 3D object lines can be determined as

$$(N_{Xi}, N_{Yi}, N_{Zi}) = (A, B, C) \times (p, q, r_i/f), \tag{1}$$

since (N_{Xi}, N_{Yi}, N_{Zi}) is perpendicular to both the surface normal vectors, (A, B, C) and $(p, q, ri/f)$, of plane W and the backprojection plane.

Therefore, the equation of the 3D object line is

$$\frac{X + qD/(qA - pB)}{N_{Xi}} = \frac{Y - pD/(qA - pB)}{N_{Yi}} = \frac{Z}{N_{Zi}} \tag{2}$$

if N_{Xi}, N_{Yi}, and N_{Zi} are all not zero.

If $N_{Xi} = 0$, X is equal to X_0. The terms in Y and Z of the line equation in Eq. (2) can be calculated. Similarly, if $N_{Yi} = 0$, Y is equal to Y_0, the terms in X and Z can also be obtained. □

Lemma 2. *Let lines L_1 and L_2 on a plane W intersect at a point H. If line $\overline{GH}$ is parallel to the image plane, then the images of L_1 and L_2, denoted by l_1 and l_2, are parallel to each other and parallel to $\overline{GH}$, too.*

Proof. As illustrated in Fig. 1, line L_1 and point G define a plane P_1, and line L_2 and point G define a plane P_2. The planes P_1 and P_2 intersect the image plane at the image lines l_1 and l_2. Since points G and H are on both planes P_1 and P_2, $\overline{GH}$ is the intersection of planes P_1 and P_2.

(a) First, we show that l_1 and l_2 are parallel to each other: Assume l_1 and l_2 are not parallel to each other. Since l_1 and l_2 are on the image plane, they intersect at a point k. Therefore, point k belongs to both planes P_1 and P_2 and is, thus, on line $\overline{GH}$. This is a contradiction to the fact that $\overline{GH}$ is parallel to and not on the image plane. So l_1 and l_2 are parallel to each other.

(b) Next, we show that l_1 and l_2 are parallel to $\overline{GH}$: Because l_1 and $\overline{GH}$ are on plane P_1, if l_1 is not parallel to $\overline{GH}$, $\overline{GH}$ intersects l_1 and, therefore, the image plane. This is a contradiction to that $\overline{GH}$ is parallel to and not on the image plane. Thus l_1 must be parallel to $\overline{GH}$. Similarly, it can be shown that l_2 is parallel to $\overline{GH}$. □

In the following, it is easy to see that the dual property is still valid in the cases of multiple parallel lines.

Lemma 3. *Let $\mathbf{g} = \{l_i \mid 1 \leqslant i \leqslant n\}$ be a set of n parallel lines in the image plane. If the object plane W is not parallel to any line in $\mathbf{g}$, then*

(a) *all the 3D corresponding lines for lines in $\mathbf{g}$ on plane W meet at a point H.*
(b) *line $\overline{GH}$ is parallel to all lines in $\mathbf{g}$ and the image plane as well.*

Proof. By Theorem 1, any two parallel lines l_i and l_j in $\mathbf{g}$ have a 3D IIP H_k. In addition, line $\overline{GH_k}$ is parallel to lines l_i and l_j and H_k is on plane W. All 3D IIP H_k must be identical since all $\overline{GH_k}$ is parallel to lines in $\mathbf{g}$ and passes the COP. Thus Lemma 3 is valid. □

Thus the 3D IIP can be estimated. Multiple parallel image lines have the same 3D IIP H on a 3D plane W, $AX + BY + CZ + D = 0$. Similar to Lemma 1, the 3D IIP is at $(-qD/(qA - pB), pD/(qA - pB), 0)$.

Lemma 4. *Let a set of 3D concurrent lines $\mathbf{G} = \{L_i \mid 1 \leqslant i \leqslant n\}$ intersect at a common point H and $\mathrm{g} = \{l_i \mid 1 \leqslant i \leqslant n\}$ be the set of their corresponding image lines. If line $\overline{GH}$ is parallel to the image plane, then lines in $\mathbf{g}$ are parallel to each other.*

Proof. Since $\overline{GH}$ is parallel to the image plane, by Lemma 2, we can obtain that l_1 in $\mathbf{g}$ is parallel to l_2, l_2 is parallel to l_3, and l_{n-1} is parallel to l_n and so on. Therefore, $l_1, l_2, \ldots,$ and l_n in $\mathbf{g}$ are parallel to each other. □

3. The dual vanishing line property

In this section, the behavior of the 3D IIPs is investigated. The 3D IIPs are shown to be collinear. This property is corresponding to the vanishing line property [5].

Lemma 5 (The dual vanishing line property). *The 3D IIPs on a 3D object plane W for all groups of parallel image lines are collinear. Besides, the collinear line is parallel to the image plane and lies on the plane of $Z = 0$.*

Proof. Let $\mathbf{g}_1, \mathbf{g}_2, \ldots,$ and $\mathbf{g}_n$ be n groups of parallel image lines. Also let H_i be the 3D IIP for group $\mathbf{g}_i$ (if $\mathbf{g}_i$ is parallel

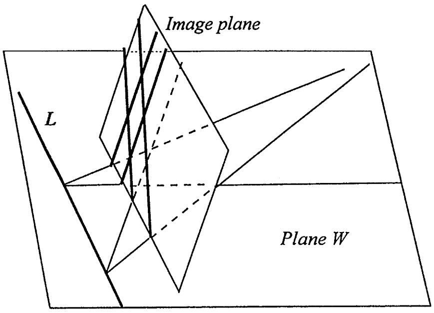

Fig. 2. The dual vanishing line property.

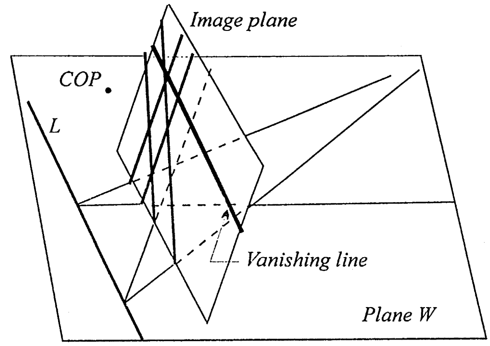

Fig. 3. Line L defined by the convergent points is parallel to the vanishing line.

to plane W, the 3D IIP is at the infinity). According to Lemma 3, $\overline{GH_i}$ is parallel to lines in $\mathbf{g}_i$ (so also parallel to the image plane) and H_i is on the plane W. Thus, all 3D IIPs H_i on plane W form a line L parallel to the image plane (see Fig. 2). The Z coordinate of all IIPs H_i is 0. Therefore, line L is on the X–Y plane. □

To express Lemma 5 in an algebraic form, let there exist n groups of parallel lines $\mathbf{g}_i$, $i = 1, \ldots, n$ on the image plane. The equations of parallel lines in group $\mathbf{g}_i$ are $p_i x + q_i y + r_{ij} = 0, i = 1, \ldots, n,$ and $j = 1, \ldots, m_i$, where m_i is the number of lines in group $\mathbf{g}_i$. All 3D object line for group $\mathbf{g}_i$ on a plane W, expressed by $AX + BY + CZ + D = 0$, has a 3D IIP H_i (Lemma 3). All IIP H_i form line L on X–Y plane whose equation is

$$L = \left\{ \begin{pmatrix} X \\ Y \end{pmatrix} \middle| AX + BY + D = 0 \right\} \quad \text{for } Z = 0.$$

Lemma 6. *The collinear line L defined by all 3D IIPs in the dual vanishing line property is parallel to the vanishing line for a plane W on the image plane.*

Proof. The equation of the vanishing line for all planes $AX + BY + CZ + D_i = 0$ is $Ax + By + Cf = 0$ [5]. Thus, the collinear line L of the 3D IIPs, $AX + BY + D = 0$, for $Z = 0$ is parallel to the vanishing line (see Fig. 3). □

We have investigated the IIPs on a unique object plane. What happens if the object planes are different for different image parallel lines. According to Lemmas 3 and 5, the following lemma is in order.

Lemma 7. *Let* $\mathbf{g}_p = \{l_{pi} \mid 1 \leqslant i \leqslant n\}$ *and* $\mathbf{g}_q = \{l_{qi} \mid 1 \leqslant i \leqslant m\}$ *be two groups of parallel image lines. Let the 3D IIP on a backprojected object plane* W_p *for* $\mathbf{g}_p$ *be point* H_p. *Also let the 3D IIP on a distinct object plane* W_q *for* $\mathbf{g}_q$ *be point* H_q. *Then line* H_pH_q *is parallel to the image plane* (Fig. 4).

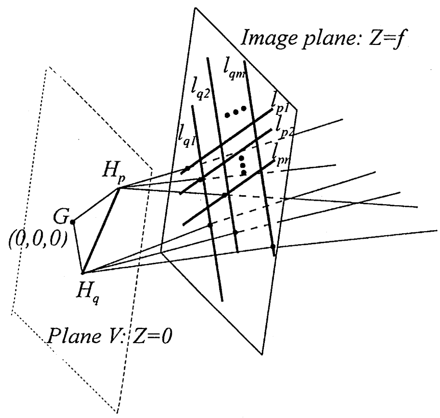

Fig. 4. Line $\overline{H_pH_q}$ is parallel to the image plane.

Example. Fig. 5(a) displays the image of a vase. Let l_{pi} and l_{qi}, for $i = 1, 2$, be two sets of parallel lines in the image. Let coplanar lines Lp_1 and Lp_2 be the 3D tangent lines corresponding to l_{p1} and l_{p2}, respectively. Also let coplanar lines Lq_1 and Lq_2 be the 3D tangent lines corresponding to l_{q1} and l_{q2}, respectively. Since the radii of the circles in space defined by the two sets of tangent points P_i and Q_i are different, the two sets of tangent lines Lp_i and Lq_i, $i = 1, 2$, are not coplanar. However, by Lemma 7, we can gain that the line defined by the two 3D IIPs of the 3D object lines Lp_i and Lq_i is parallel to the image plane (Fig. 5(b)).

Lemma 8. *The 3D IIPs on different object planes for different groups of parallel image lines lie on a common plane V. The plane V is parallel to the image plane. In addition, it passes through the COP.*

Proof. According to Lemma 7 and its proof, any two groups of parallel image lines have 3D IIPs H_i and H_j on a plane V defined by $\overline{GH_i}$ and $\overline{GH_j}$. Thus, plane V is parallel to the image plane (see Fig. 4) and also passes point G (the COP) since $\overline{GH_i}$ and $\overline{GH_j}$ are parallel to the image plane, respectively. □

According to Lemma 8, the equation of plane V is $Z = 0$.

Up to now, the dual properties of the vanishing point and vanishing line have been established. In the following sections, a general model for the 3D intersection inference from image lines is illustrated and two applications of the dual properties are given.

4. A general model for the 3D line intersection inference from their image lines

In this section, we examine the properties between the 3D lines and their corresponding image lines. First, If 3D lines are parallel, then their image lines generally intersect at a vanishing point on the image plane. If the 3D lines are not parallel, then their image lines may or may not intersect at an intersection point. Furthermore, the intersection point (or the extrapolated one) on the image plane may or may not correspond to the real 3D intersection point (if there is one). A general model for the 3D line inference from their image lines will be given, no matter whether the 3D lines are parallel or non-parallel. In the following, we start with the projections of the 3D coplanar, but non-parallel lines, then the projections 3D of non-coplanar lines.

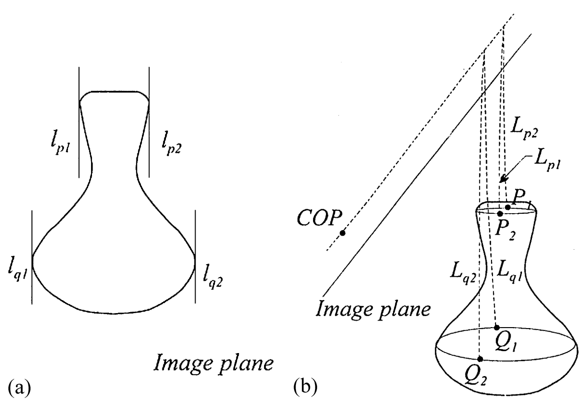

Fig. 5. (a) The image of a vase and parallel tangent lines; (b) The 3D convergent points.

4.1. Projections of 3D coplanar lines

Let $\overline{AB}$ and $\overline{CD}$ be two 3D coplanar, but non-parallel line segments on a plane. It will be pointed out that unless the image lines of the 3D coplanar lines intersect at an internal point, the extended intersection point of the image lines may not be the projection of the true intersection point of the 3D coplanar lines. As shown in Fig. 6, point E is closer to point B (or D) than point A (or C). Let line segments $\overline{ab}$ and $\overline{cd}$ be the projections of $\overline{AB}$ and $\overline{CD}$. There are three different projection types for the images of $\overline{AB}$ and $\overline{CD}$.

Type C1 (*True intersection*). *If the intersection point, e, of the extended line segments $\overline{ab}$ and $\overline{cd}$ is the projection of the true intersection point E, then the image lines are said to be of Type C1.*

In this case, point e is closer to point b (or d) than point a (or c).

Type C2 (*Parallel case*). *If line $\overline{ab}$ is parallel to line $\overline{cd}$, and therefore, the true intersection point E has no corresponding image point, then the image lines are said to be of Type C2.*

This case implies that the projected lines of two intersecting lines are parallel. According to Lemma 2, this is the case if line $\overline{GE}$ is parallel to the image plane.

Type C3 (*False intersection*). *If the intersection point k of the two extended line segments $\overline{ab}$ and $\overline{cd}$ is not corresponding to the true intersection point, then the image lines are said to be of Type C3.*

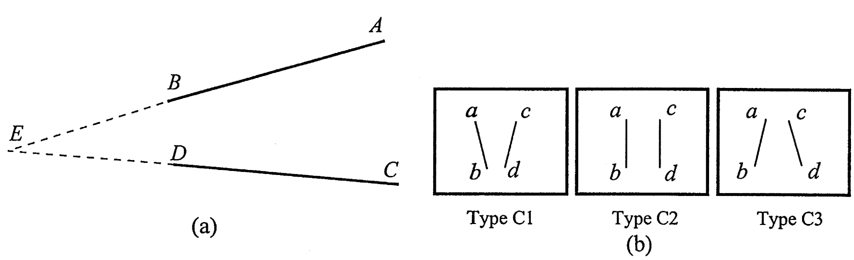

Fig. 6. (a) Coplanar non-parallel line segments intersect at a point when extended. (b) Three types of images for (a).

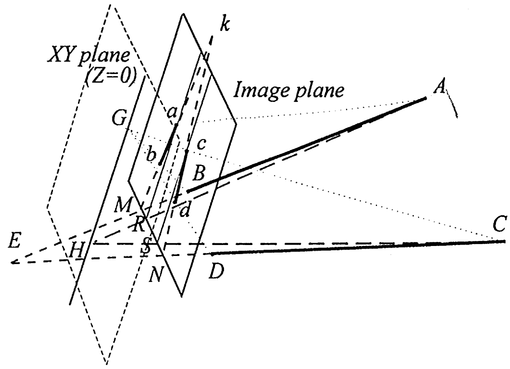

Fig. 7. The projection geometry of Type 3.

Type C3 is difficult to visualize without the aid of the above lemmas. Consider the case where point E is located behind the X–Y plane (i.e., the plane at $Z = 0$), as shown in Fig. 7. Assume there exists a point H, on the X–Y plane, in-between $\overline{AE}$ and $\overline{CE}$ such that line $\overline{GH}$ is parallel to the image plane. Let points R and S be the intersection points of lines $\overline{AH}$, $\overline{CH}$ with the image plane, respectively. Since $\overline{GH}$ is parallel to the image plane, by Lemma 2, we know that the projection lines, $\overline{aR}$ and $\overline{cS}$, of lines $\overline{AH}$ and $\overline{CH}$ are parallel.

Let line $\overline{MN}$ be the intersection line between plane $ABCD$ and the image plane, and let points M and N be the respective intersection points of lines $\overline{AB}$, $\overline{CD}$ with the image plane. Since point H is located between lines $\overline{AB}$ and $\overline{CD}$, points R and S must be located between points M and N. Line $\overline{aR}$ is parallel to line $\overline{cS}$, so $\overline{ab}$ (or $\overline{aM}$) and $\overline{cd}$ (or $\overline{cN}$) must be non-parallel lines and intersect at a point k. Point k is closer to point a (and c) rather than point b (and d). However, $\overline{AB}$ and $\overline{CD}$ will not have a second intersection except point E. Therefore, point k cannot be the correct projection of the true intersection point E. Note that in this case, the closeness between the 3D spatial points (e.g. between B and D) is just opposite to the relation between their corresponding 2D image points.

Let the X–Y–Z coordinate system be defined as before. Now, based on the above dual properties, a general perspective projection model for 3D coplanar lines can be summarized as follows: (1) If the intersection point E is located in front of the X–Y plane (i.e., the Z coordinate of point E is positive), the line projections is of Type C1. (2) If point E is on the X–Y plane, then the line projection is of Type C2. (3) A Type C3 case occurs if point E is located behind the X–Y plane (i.e., the Z coordinate of point E is negative).

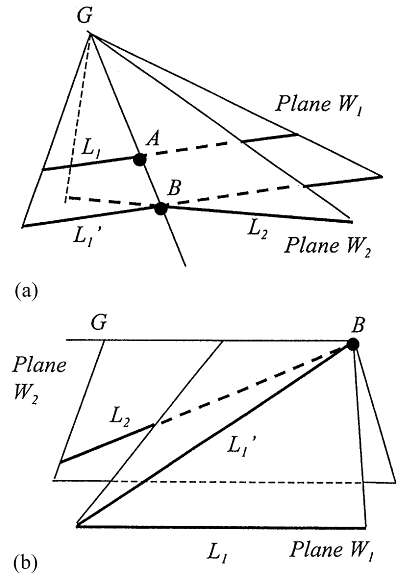

Fig. 8. (a) Common projection ray for non-coplanar lines. (b) Projections of non-coplanar lines in Case 2.

4.2. Projections of 3D non-coplanar lines

The projections of non-coplanar lines are seldom discussed. Using the properties and projection types mentioned above, we can formulate this problem as follows.

Let L_1 and L_2 be two non-coplanar lines. They must be neither parallel nor intersecting. Let point G (the COP) and L_1 define plane W_1, and point G and L_2 define plane W_2 (see Fig. 8(a)). Since lines L_1 and L_2 are not parallel, there are two general cases of L_1 and L_2 with respect to the intersection line between planes W_1 and W_2. In case 1 both lines L_1 and L_2 are not parallel to the intersection line; assume L_1 intersects plane W_2 at point A and line L_2 intersects plane W_1 at point B, as shown in Fig. 8(a). In case 2 only one of the lines L_1 and L_2 is not parallel to the intersection line; assume arbitrarily line L_2 intersects plane W_1 at point B, as shown in Fig. 8(b).

In Case 1, since points G, A, and B belong to both planes W_1 and W_2 (i.e., on the intersection line of the two planes), the projections of points A and B will be identical. The backprojection rays $\overline{GA}$ and $\overline{GB}$ are collinear, so it is referred to as the *common backprojection ray* for points A and B on lines L_1 and L_2, respectively. There also exists a line L_1' on plane W_1 which is parallel to line L_1 and intersects L_2 at point B (see Fig. 8(a)). The projections of L_1 and L_2 are the same as the projections of coplanar lines L_1' and L_2. Using the common backprojection ray, we can convert the projections of non-coplanar lines to the projections of non-parallel lines on the same plane as mentioned in the above subsection. According to the three projection types described in Section 4.1, the projections of L_1 (or L_1) and L_2 are parallel if line $\overline{GB}$ is parallel to the image plane. On the other hand, the projections of L_1 and L_2 may have an intersection point that is either a real intersection or a false intersection. If point B is in front of the plane $V(Z = 0)$, the image of the object lines is of Type C1. If point B is behind the plane $V(Z = 0)$, the image is of Type C2.

Case 2 is similar to Case 1. Let L_1' be a line on plane W_1 and pass through point B (see Fig. 8(b)). Since L_1' is coplanar with L_1, the possible projections of lines L_1 and L_2 are the same as the projections of lines L_1' and L_2. As a result, Case 2 can be converted to the projections of coplanar lines. There are three types of projections depending on the position of point B.

Up to now, a general model for the perspective projections of arbitrary lines (coplanar or non-coplanar) has been established. Based on the above results, the geometric reasoning of the 3D lines in an image can be done next.

4.3. 3D line intersection inference

For presentation convenience, we consider only the case of two image lines. The case of multiple image lines can be obtained in a similar manner. Also, assume the 3D objects producing the image lines are lines. The case in which an image line is projected from a curve or multiple lines is out of the scope of this study.

4.3.1. The case of parallel image lines

If the image lines are parallel, there are three possible combinations of the corresponding 3D object lines:

1. *The 3D lines are parallel* (this is the case when the 3D object plane is parallel to the image lines);
2. *The 3D lines have a 3D IIP* (this is true if the object plane is not parallel to the image lines);
3. *The 3D lines are neither parallel nor intersecting* (this is the case when the corresponding 3D lines of the image line do not belong to the same plane, as discussed in Section 4.2).

4.3.2. The case of non-parallel image lines

If the image lines are not parallel, they must have either an apparent intersection point p (i.e., the two image lines intersect at an internal point) or an extrapolated intersection point p (i.e., the two image lines intersect after they are extended). The 3D line intersection properties for such non-parallel image lines can be inferred as follows.

(1) For the case of an apparent intersection point p, there are two situations of the 3D lines:
   (a) *The 3D lines are coplanar and intersect*,
   (b) *The 3D lines are non-coplanar* (this is the case when one object line is occluded by another object line).

(2) For the case of an extrapolated intersection point p, there are three situations for the 3D lines.
   (a) *The 3D lines are coplanar and parallel.* Point p is the vanishing point;
   (b) *The 3D lines are coplanar and intersect if extended* (this is the case when the image is of Type C1 or of Type C3);
   (c) *The 3D lines are non-coplanar*, as discussed in Section 4.2.

5. The 3D pose parameters of a circle using a set of two parallel image lines

In this section, we show the use of the dual property in determining the 3D pose parameters of a circle. Due to the perspective distortion, this problem is not easy as it appears. Kanatani and Liu [12] used a matrix transformation technique to convert a circle image into a regular type with the ellipse center at the image center and the major and minor axes on the horizontal and vertical axes of the image plane, respectively. This regular type image is then converted again into a circular one by applying another transformation. Therefore, the pose parameters associated with the final circular image can be estimated by using matrix trace properties. Finally, Kanatani and Liu used inverse transformations to obtain the original pose parameters of the circle.

Here, the solution process can be simplified. It resolves the 3D pose parameters directly from the typical type of circle images without the extra transformation into a circular one and without the usage of the matrix transformation. In this method, the surface orientation of the circle is a geometric solution with a clear geometric interpretation.

Fig. 9 depicts the typical type of circle image (an ellipse). The major axis $\overline{pq}$ of the ellipse is on the x-axis of the image plane and the minor axis $\overline{bc}$ is on the y-axis. It is readily shown that the tangent lines l_1 and l_2 to the endpoints of the major axis $\overline{pq}$ is parallel to each other

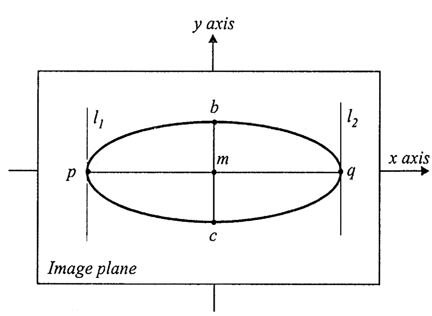

Fig. 9. The canonical image of a circle.

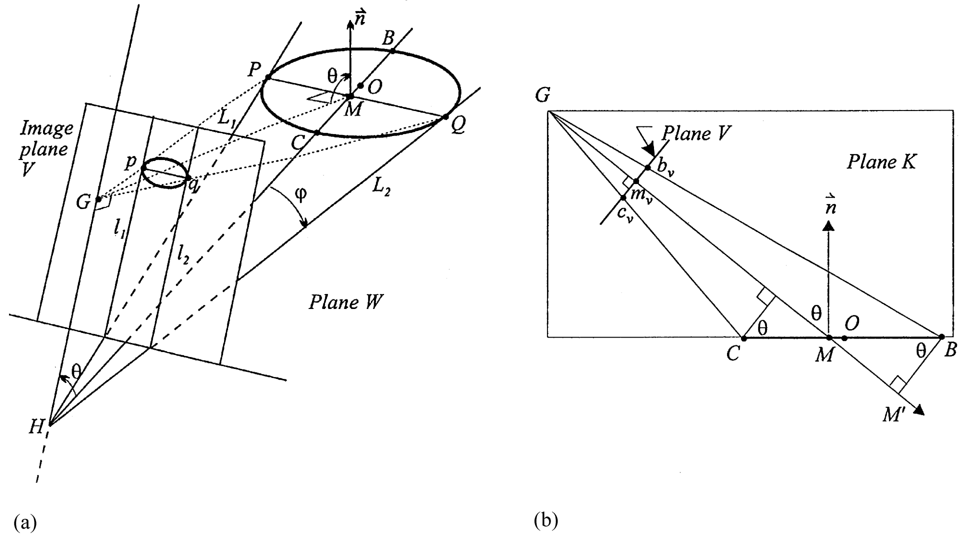

Fig. 10. (a) The perspective projection of the canonical image. (b) The images of the circle on the Y–Z plane.

and parallel to the y-axis, too. We will establish the relations between the parallel tangent lines and their corresponding 3D lines by the dual property. Here we show how to solve the orientation of the circle. The position center of the circle can then be obtained easily.

According to the dual vanishing point property, the corresponding 3D lines of the parallel tangent lines l_1 and l_2 will have a 3D IIP H as shown in Fig. 10(a). Define the camera (X–Y–Z) coordinate system and the image (x–y) coordinate system as above. Since the circle image is symmetrical around the y-axis, the circle is symmetrical around the Y–Z plane and points P and Q are symmetrical around the Y–Z plane. Therefore, the surface normal **n** of the circle with respect to the X–Y–Z coordinate system can be expressed as

$$\boldsymbol{n} = (0, \sin\theta, -\cos\theta),$$

where θ is the angle between vector $\boldsymbol{n}$ and the camera optical axis (the Z-axis), and $0° \leqslant \theta \leqslant 90°$.

Let $\overline{PQ}$ and $\overline{BC}$ be the 3D corresponding chords of $\overline{pq}$ and $\overline{bc}$, and points M and m be the center points of $\overline{PQ}$ and $\overline{pq}$, respectively. Also let φ be the angle between $\overline{HM}$ and $\overline{HP}$ (or $\overline{HQ}$). Lines $\overline{GM}$ (the camera optical axis) and $\overline{HM}$ will be perpendicular to and bisect $\overline{PQ}$ since they are on the Y–Z plane.

After applying the dual property of the vanishing point, as shown in Fig. 10(a) and (b), we can set up four equations, i.e., Eqs. (3)–(6), in four unknowns θ, φ, $|\overline{PQ}|$, and $|\overline{GM}|$ as follows. Correspondingly, θ can be solved.

$$\frac{|\overline{pq}|}{f} = \frac{|\overline{PQ}|}{|\overline{GM}|} \quad \text{for } \Delta\, Gpq \text{ is similar to } \Delta GPQ, \tag{3}$$

where f is the effective focal length.

$$\tan\varphi = \frac{|\overline{PM}|}{|\overline{HM}|} = \frac{|\overline{PQ}|/2}{|\overline{GM}|/\sin\theta} = \frac{|\overline{pq}|\sin\theta}{2f} \tag{4}$$

and

$$R\cos\varphi = |\overline{PQ}|/2 \quad \text{where } R \text{ is the given circle radius.} \tag{5}$$

In addition, from the similar triangles ΔGmb and $\Delta GM'B$, we attain

$$\frac{|\overline{bm}|}{|\overline{BM'}|} = \frac{|\overline{Gm}|}{|\overline{GM'}|}, \text{ or } \frac{|\overline{bm}|}{R(1+\sin\varphi)\cos\theta} = \frac{f}{|\overline{GM}| + R(1+\sin\varphi)\sin\theta}, \tag{6}$$

since $|\overline{BM'}| = |\overline{BM}|\cos\theta$ and $|\overline{BM}| = R(1+\sin\varphi)$. From Eq. (4),

$$\sin\varphi = |\overline{pq}|\sin\theta/\sqrt{4f^2 + |\overline{pq}|^2\sin^2\theta} \tag{7}$$

and

$$\cos\varphi = 2f/\sqrt{4f^2 + |\overline{pq}|^2\sin^2\theta} \tag{8}$$

Also, from Eq. (3),

$$|\overline{GM}| = \frac{f|\overline{PQ}|}{|\overline{pq}|} = \frac{2fR\cos\varphi}{|\overline{pq}|} = \frac{2fR}{|\overline{pq}|}\frac{2f}{\sqrt{4f^2 + |\overline{pq}|^2\sin^2\theta}} \quad (9)$$

Eq. (6) can be rewritten as $fR(1+\sin\varphi)\cos\theta = |\overline{bm}|(|\overline{GM}| + R(1+\sin\varphi)\sin\theta)$. It can then be expressed in terms of θ by applying Eqs. (7)–(9).

$$R(1+\sin\varphi)(f\cos\theta - |\overline{bm}|\sin\theta) = |\overline{bm}|\frac{2fR\cos\varphi}{|\overline{pq}|}.$$

After some rearrangement,

$$|\overline{pq}|^2(f^2 + |\overline{bm}|^2)\sin^2\theta = f^2(|\overline{pq}|^2 - 4|\overline{bm}|^2).$$

Thus,

$$\sin\theta = \pm\frac{f}{|\overline{pq}|}\sqrt{\frac{|\overline{pq}|^2 - 4|\overline{bm}|^2}{f^2 + |\overline{bm}|^2}}.$$

Therefore, θ and the orientation of the circle can be obtained by using the dual property. Besides, the surface orientation **n** of the circle is a function of the lengths of the major and the minor axes, i.e., $|\overline{pq}|$ and $|\overline{bc}|(=2|\overline{bm}|)$. Once **n** bar is obtained, the position of the center of the circle can also be derived easily.

6. The camera setup in a binocular vision system using six specially designed 3D lines

Here the new theory is applied to set up two cameras on a fixture (e.g., or on a robot head). The two cameras will be adjusted such that (1) the relationship between the cameras and the fixture meets a special geometry (for instance, both the camera optical axes are perpendicular to a special plane) and (2) the epipolar line for any spatial point can be located readily in the two images.

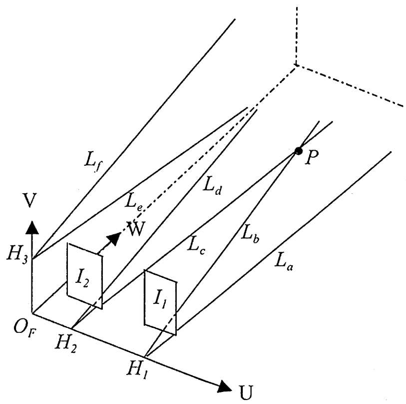

Fig. 11. Calibration setup in a stereo vision system.

We demonstrate new a simple vision-based method to achieve the above two goals. In Fig. 11, two cameras are to be set up on a fixture such that both the camera optical axes are perpendicular to a special plane (the U–V plane to be defined next). Let the three axes of the fixture coordinate system be the U, V, and W axes with the origin at point O_F. Let L_a, L_b, L_c, L_d be four coplanar lines on the U–W plane and coplanar lines L_e and L_f on the V–W plane. Furthermore, there are three non-collinear points H_1, H_2, and H_3 on the U–V plane where points H_1 and H_2 are on the U-axis and H_3 is on the V-axis. Let lines L_a and L_b intersect at point H_1; lines L_c and L_d intersect at H_2; and lines L_e and L_f intersect at H_3, respectively. Besides, L_a is parallel to L_c and L_b is parallel to L_d. Also assume only lines L_b and L_c intersect at point P in front of the U–V plane. Assume both cameras are located above the U–W plane and to the right of the V–W plane. The cameras are so arranged that lines L_a, L_b, L_c, L_d, L_e, and L_f are all visible. The images of L_a, L_b, L_c, and L_d are denoted by l_{ak}, l_{bk}, l_{ck}, and l_{dk} on image plane I_k, for $k = 1$ or 2, respectively. Lines l_{ak} and l_{ck} define a vanishing point v_{1k} and lines l_{bk} and l_{dk} define another vanishing point v_{2k}. Let the camera coordinate systems of the two cameras be defined as before, i.e., X_k–Y_k–Z_k coordinate systems, $k = 1, 2$. Initially, the X_k, Y_k, and Z_k axes are roughly in the U, V and W directions and the COPs of both cameras are located behind the U–V plane. (The plane $Z_k = 0$ contains the COP and is parallel to the image plane I_k.)

Fig. 12 shows an image of the three line pairs. The correspondences between l_{ak}, l_{bk}, l_{ck}, l_{dk}, l_{ek}, l_{fk} and L_a, L_b, L_c, L_d, L_e, L_f can be easily found using the image of the sole intersection point P and the line adjacency relation. After the line correspondences are found, we attempt to accomplish the goal set at the outset, namely to arrange plane $Z_k = 0$, $k = 1, 2$, to coincide with the U–V plane which contains points H_1, H_2, and H_3. We can design a procedure for the camera arrangement based on Lemma 5 (or Lemma 8). Basically, if the plane $Z_1 = 0$ (or $Z_2 = 0$) is moved toward the U–V plane such

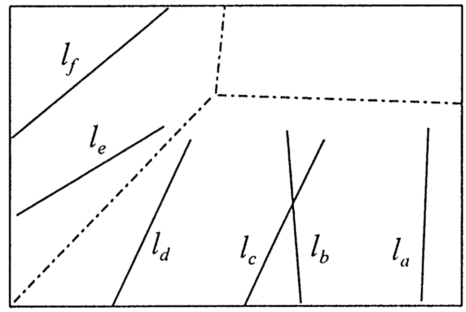

Fig. 12. An image of the six lines.

that it contains H_1 (or H_2), the resultant image lines l_a and l_b (or l_c and l_d) will become parallel to each other. If image lines l_a and l_b (or l_c and l_d) are not parallel, it implies that point H_1 (or H_2) is either in front of the plane $Z_k = 0$ or behind the plane. If H_1 (or H_2) is in the front, the two image lines will converge downward in the image; otherwise, the two image lines will converge upward. To be more precise, the image plane adjustment is carried out in the following way. First, the plane $Z_1 = 0$ is translated along the W direction such that image lines l_a and l_b become parallel. By Theorem 1, H_1 is located on plane $Z_1 = 0$. Next, to make image lines l_c and l_d parallel, camera 1 is rotated around an axis passing through H_1 and parallel to the V-axis. The rotation is made such that the resultant image lines l_c and l_d become more and more parallel. In this way plane $Z_1 = 0$ can be adjusted gradually to contain both points H_1 and H_2. Finally, if the image lines l_e and l_f are not parallel, the camera is rotated around an axis passing through H_1 and H_2. The rotation is intended to make l_e and l_f parallel. Note that during the above camera adjustment process, the actual process may not be perfect, so the camera adjustment done at a latter stage may damage the result obtained at an early stage, However, the damage can be generally kept small. The process can be repeated to bring the plane $Z_1 = 0$ to a final position such that it contains H_1, H_2, and H_3. Similarly, the plane $Z_2 = 0$ can be also made to contain H_1, H_2, and H_3. By doing so, both, the resultant planes $Z_1 = 0$ and $Z_2 = 0$ become parallel. Next, we will make the X_k and Y_k axes, $k = 1, 2$, be parallel to the respective U and V axes as follows. Since the vanishing line passing v_{1k} and v_{2k}, $k = 1, 2$, is parallel to the U-axis (Lemma 6), so the two vanishing lines are parallel. In each image adjust the X_k axis to be parallel to its vanishing line. At this moment, the three axes of each camera coordinate system are parallel to the three axes of the fixture coordinate system. If the focal lengths are the same (this is generally the case in a stereo vision system), the two image planes become coplanar.

We can find the 3D position of the two COPs as follows. By Theorem 1, line $\overline{G_kH_1}$ (or $\overline{G_kH_2}$) is parallel to lines l_{ak} and l_{bk} (or l_{ck} and l_{dk},), for $k = 1$ or 2. Since the axes of the camera and the fixture coordinate systems are parallel and the coordinates of point H_i are known, the position of the COP (G_k) in the U–V–W coordinate system can then be calculated by intersecting two lines of $\overline{G_kH_1}$ and $\overline{G_kH_2}$, for $k = 1, 2$.

Finally, either camera can be translated along the V direction to make the V coordinate of the COP G_1 equal to that of the COP G_2. As a consequence, the baseline of the stereo vision becomes the common X-axis. In this final parallel stereo vision system the epipolar line for a point in raw i of one image will be in the ith raw of the other image. Thus this method directly achieves the goals by using the theory about the projections of six spatial lines with the given special configuration.

7. Conclusion

First, we study the dual vanishing point property. Theorem 1 shows that (1) the 3D corresponding lines of two parallel lines has an IIP (inferred intersection point), and (2) the line defined by the COP and the IIP is parallel to the image plane. Then the analysis is successfully extended to multiple groups of parallel image lines. Next, the 3D IIPs on a plane for any parallel image lines are shown to be collinear. This is named the dual vanishing line property. Some related properties are then given.

Based on the derived properties, we study three possible projection types (Types C1–C3) of coplanar lines in 3D space. We then give a general model for the 3D line intersection inference from their image lines. Finally, we give two applications of the usage of the new results. One is to determine the 3D pose parameters of a circle using two parallel image lines and the other is to set up the cameras in a standard binocular vision system using six special 3D lines.

References

[1] S.-C. Pei, L.-G. Liou, Rigid motion and structure from several sets of parallel lines in a monocular image sequence, Pattern Recognition 27 (11) (1994) 1475–1491.

[2] L. Cremona, Introduction to Projective Geometry, Dover, New York, 1913.

[3] Young, J. Wesley, Perspective Geometry, La-Sall, Open Court, 1929.

[4] S.T. Barnard, Interpreting perspective image, Artif, Intell. 21 (1983) 435–462.

[5] R.M. Haralick, Computer and Robot Vision, Addison-Wesley, New York, 1993.

[6] S. Sull, N. Ahuja, Integrated 3-D analysis and analysis-guided synthesis of flight image sequences, IEEE Trans. Pattern Anal. Mach. Intell. 16 (4) (1994) 357–372.

[7] N.W. Campbell, M.R. Pout, M.D.J. Priestly, E.L. Dagless, B.T. Thomas, Autonomous road vehicle navigation, Eng. Appl. Artif. Intell. 7 (3) (1994) 177–190.

[8] T. Stahs, F. Wahl, Recognition of polyhedral objects under perspective views, Comput. Artif. Intell. 11 (2) (1992) 155–172.

[9] S. Li shigang, S. Tsuji, M. Imai, Determination of 3-D structure using lines viewed by a moving camera, Systems Comput. in Jpn 23 (7) (1992) 24–55.

[10] K. Liu, R. Jiang, Y.-Q. Cheng, J.-Y. Yang, Camera calibration based on coplanar points, Proc. SPIE: Soc. Opt. Eng. 1820 (1993) 16–24.

[11] L.L. Wang, W.-H. Tsai, Camera calibration by vanishing lines for 3-D computer vision, IEEE Trans. Pattern Anal. Mach. Intell. 13 (4) (1991) 370–376.

[12] K. Kanatani, W. Liu, 3D interpretation of conics and othogonality, CVGIP: Image Understanding 58 (3) (1993) 286–301.

About the Author—JEN-BIN HUANG recieved the B.S. and M.S. degrees in electrical engineering from National Cheng-Kung University, Taiwan, Republic of China, in 1984 and 1986, respectively. He is currently a Ph.D. candidate in computer science and information engineering from National Chiao-Tong University, in Taiwan. Prior to his Ph.D. program he worked for Advantech Inc. from 1990 to 1992 and Chung-Shan Institute of Science Technology from 1986–1990, respectively. His research interests include computer vision, system engineering, virtual reality, human interface, image processing, and parellel system.

About the Author—ZEN CHEN recieved the B.Sc. degree from National Taiwan University in 1967, the M.Sc. degree from Duke University in 1970, and the Ph.D. degree from Purdue University, he worked for Burroughs Corporation, Detriot, MI, where he was engaged in the development of document recognition systems. He joined National Chiao University, Taiwan, in 1974 and served as the director of the Institute of Lawrence Berkeley Laboratory, University of California, Berkeley, CA, as a visiting scientist. He was a visiting professor at the center for automation Research, University of Maryland, College Park, MD, from August 1989 to January 1990. His current research interests include computer vision, pattern recognition, virtual reality, and parellel algorithms and architectures. Dr. Chen is a member of Sigma Xi and Phi Kappa Phi. He was the founding president of the Chinese Society of Image Processing and Pattern Recognition in Taiwan. He received the outstanding engineering professor award from the Chinese Institute of Engineers in 1998.

About the Author—JENN-YIH LIN was born on 3 December 1959 in Taiwan, Republic of China. He recieved the B.Sc. Degree in control engineering in 1981, M.S. degree in computer engineering in 1986, and Ph.D. degree in 1997, all from National Chiao Tung University, Taiwan. During 1983–1984, he worked in Mechanical Industry Research Laboratories, Industrial Technology Research Institute (MIRL, ITRI) at Hsinchu as a software engineer. From 1986 to 1990, he worked as a research assistant in the Chung-Shan Institute of Technology. Currently, he is an associate professor at Ming-Hsin Institute of Technolgy. His current research interests include image processing, computer vision, optical character recognition and parallel processing.